Chapter 3
Radiofrequency Lumbar Facet Joint Denervation

Charles A. Gauci

Lumbar Facet Joint Pain

Pain originating from the facet or zygapophyseal joints is responsible for about 15 % of all low back pain complaints [1].

The facet joints are true synovial joints and pain can be precipitated by various causes such as facet joint degeneration, intervertebral disc degeneration, postural abnormalities such as lumbar scoliosis, and problems arising from the bony structures such as collapse (due to osteoporosis or pathological fractures) or defects (e.g., spondylolisthesis). It can also come about as the result of repeated minor trauma.

These conditions result in arthritic changes in the facet joints, which in turn leads to inflammation and swelling. This stretches the joint capsule and creates pain.

Clinically, the patient presents with axial low back pain which is ill-defined and poorly localized with frequent vague (i.e., nonsegmental) radiation into the groin or thigh.

It tends to be posture-related and is usually worse at rest (sitting/standing) but helped by mobility. The pain can be quite bad at night and is frequently accompanied by early morning pain and/or stiffness.

On examination, the patient exhibits pain on extension, rotation, and lateral flexion of the lumbar spine; there is frequently tenderness over the affected facet joint(s) although this may be difficult to elicit in a well-built muscular patient. Sometimes there is hypersensitivity to light touch over the painful area.

In the absence of any concomitant pathology such as a prolapsed intervertebral disc, there are usually no abnormal neurological findings or specific changes on the MRI scan.

Degenerative changes of the joints themselves may or may not be seen on imaging, but there is no correlation between the degree of any degeneration and the pain.

C.A. Gauci, MD, KHS, FRCA, FIPP, FFPMRCA
Department of Pain Management, Whipps Cross University Hospital, London E11, UK
e-mail: charles.gauci@btinternet.com

P.P.M. Menchetti (ed.), *Minimally Invasive Surgery of the Lumbar Spine*,
DOI 10.1007/978-1-4471-5280-4_3, © Springer-Verlag London 2014

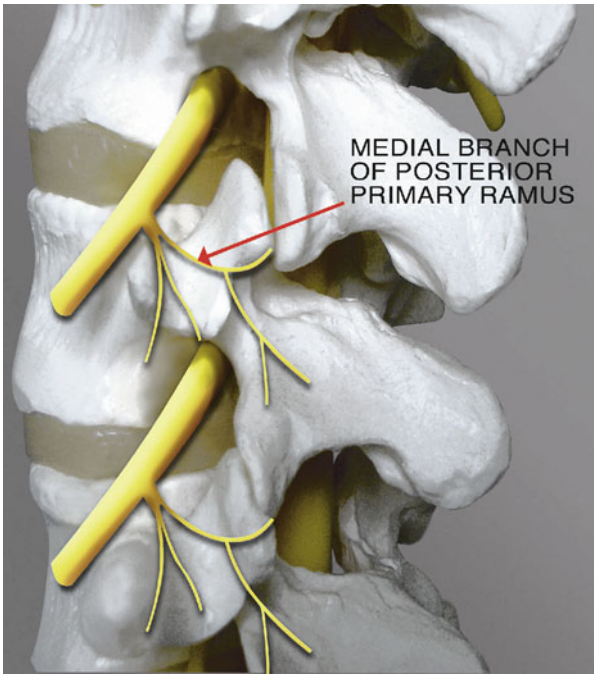

Fig. 3.1 Medial branch, lumbar posterior primary ramus

The diagnosis is made on the basis of the history, examination, and a diagnostic block, done under X-ray control.

The diagnostic block can be either an intra-articular block or, preferably, a medial branch block, using a short-acting local anesthetic such as 2 % lidocaine.

A positive diagnostic block is essential for reaching a diagnosis [2].

Radiofrequency (RF) facet denervation is currently considered the standard treatment of facet-mediated persistent pain [3].

Lumbar Facet Joint Denervation

There are various techniques used to carry out lumbar facet joint denervation.

The following description is reproduced with permission from *Manual of RF Techniques, 3rd Edition*, by Dr. Charles A. Gauci and published by CoMedical, the Netherlands, 2011.

Anatomy

Be very familiar with the medial branch of the posterior primary ramus—this is your target! (Fig. 3.1)

Table 3.1 For facet denervation, target the medial branches at the levels you want to treat together with the medial branch to the level above

Facet joint	Target medial branches of posterior primary rami of
L1/L2	T12, L1, L2
L2/L3	L1, L2, L3
L3/L4	L2, L3, L4
L4/L5	L3, L4, L5
L5/S1	L4, L5, S1

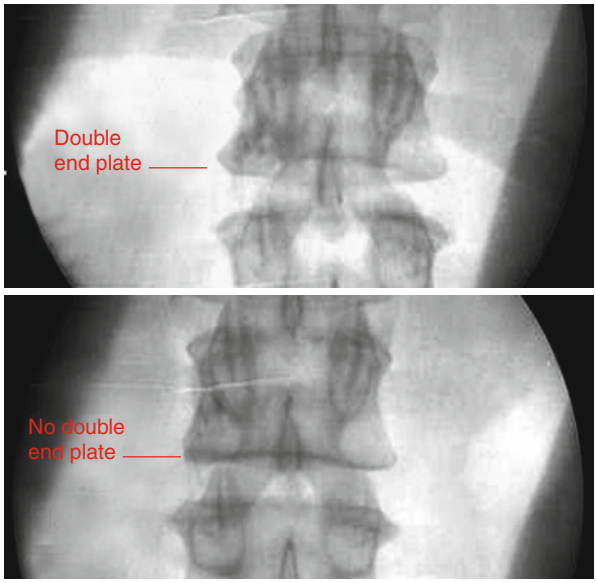

Fig. 3.2 Posteroanterior X-ray view of lumbar spine showing double end plate and its plate removal

For facet denervation, target the medial branches at the levels you want to treat together with the medial branch to the level above (Table 3.1).

Position of Patient

The patient should be lying prone on a radiolucent table; stand on the left side of the patient if you are right-handed and vice versa if you are left-handed.

With the C-arm image intensifier in the posteroanterior axis, obtain a clear view of the lumbar vertebrae; if necessary, adjust the position of the image intensifier so as to obliterate any double end plates. It is done by angling the image intensifier, which is in the posteroanterior axis, very slightly caudally. This maneuver results in the lower border becoming a single line on X-ray screening (Fig. 3.2). Occasionally, the double end plate is removed by moving the axis of the C-arm image intensifier very slightly cranially.

The best place to start trying to locate the medial branch of the posterior primary ramus is the point where it enters the groove on the back of the vertebral lamina.

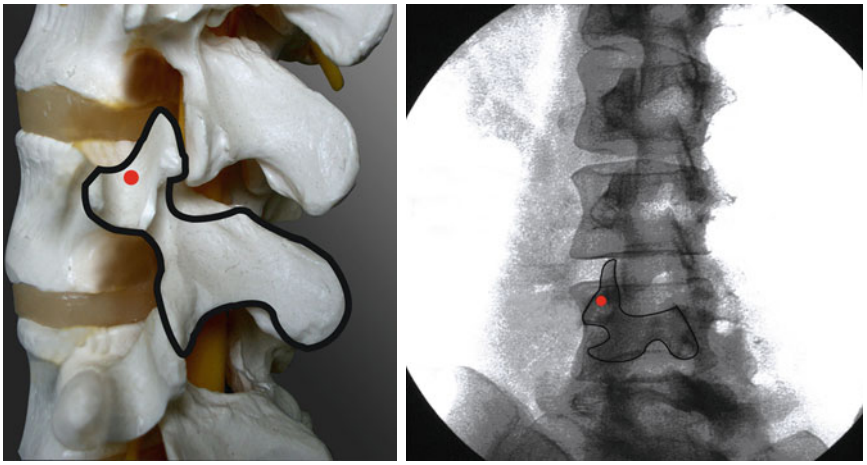

Fig. 3.3 "Eye of the Scottie dog"

Fig. 3.4 Target!

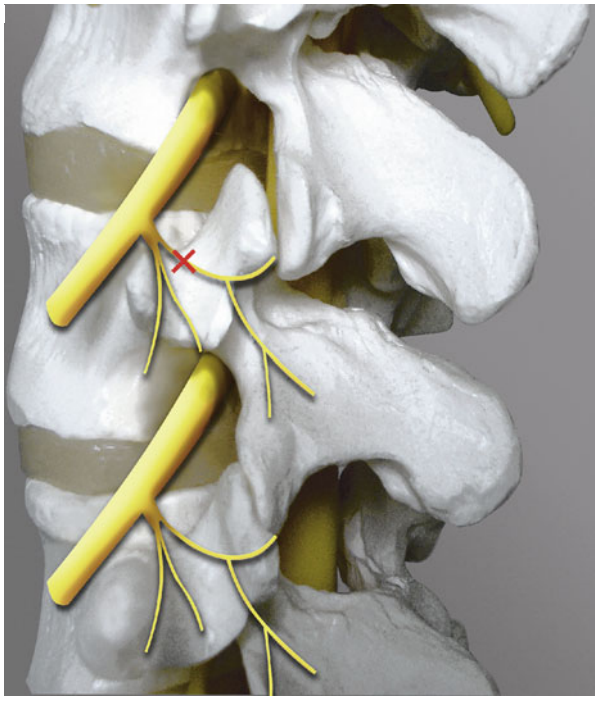

For this you need to move the image intensifier from its initial posteroanterior axis (corrected for "double end plates") obliquely away from the patient so as to obtain a good view of the so-called Scottie dog. Your preliminary target is the "eye of the dog" (Fig. 3.3); this point overlies the medial branch (Fig. 3.4).

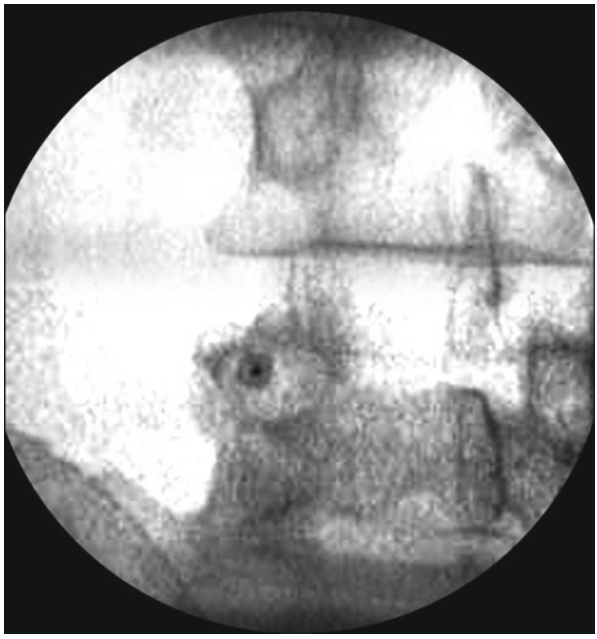

Fig. 3.5 Tunnel vision

Technique

Use a 25# needle to infiltrate the superficial tissues only; do not go down as far as bone, as you will anesthetize the medial branch and be unable to locate it by stimulation.

Insert a 22#, 100.5 mm (5 mm exposed tip) RF needle along the angle of the X-ray beam so as to hit the "eye of the Scottie dog" in tunnel vision (Fig. 3.5).

Replace the RF needle stilette with the thermocouple electrode and try to locate the medial branch by sensory stimulation, using the following parameters on your machine:

Frequency: 50 Hz
Pulse width: 1 ms
Voltage: up to 0.5 V

NB if you only manage to locate the nerve at a voltage greater than 0.5 V, keep looking! You are unlikely to produce an effective lesion here.

If you cannot locate the nerve on bone, then slip forward off bone and into the groove close to the intervertebral foramen (Fig. 3.6) and try again. If you still cannot locate the nerve, advance deeper *and very slowly* checking the position of your needle in the lateral axis (Fig. 3.7). The tip of your needle must *never* lie anterior to an imaginary line passing through the posterior margin of the intervertebral foramen (Fig. 3.8). *If you lesion anterior to this point, you run the double risk of causing neuritis and of damaging the motor root.*

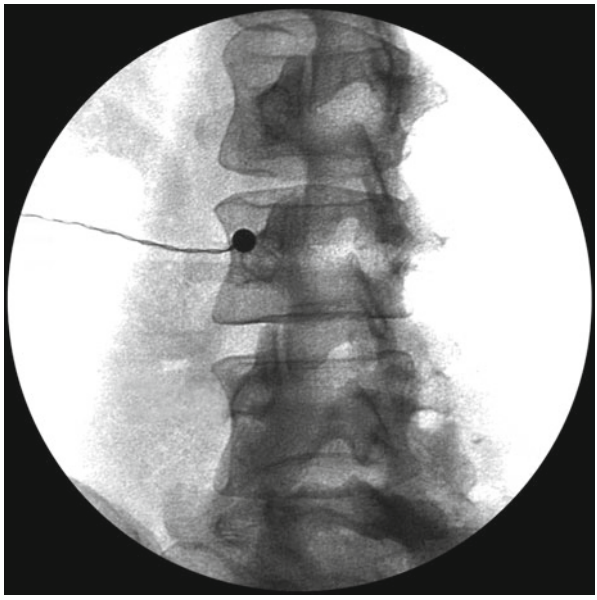

Fig. 3.6 Needle in groove

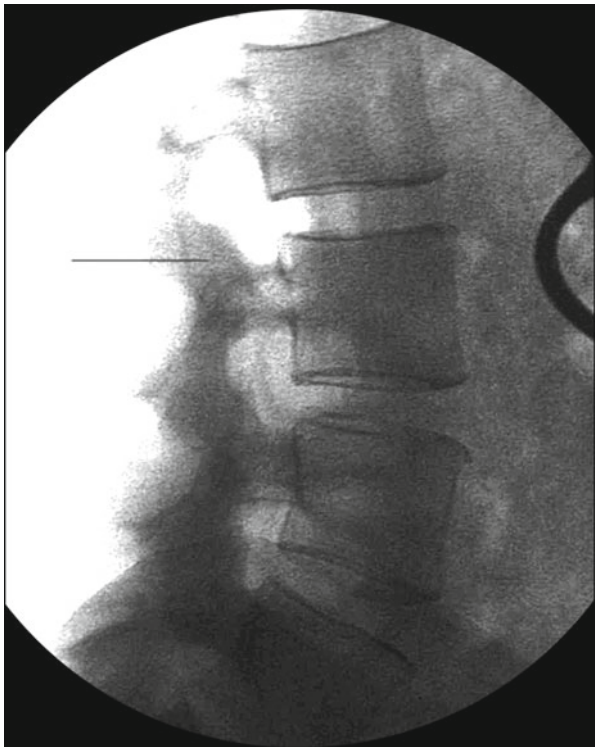

Fig. 3.7 View of needle in lateral axis-1

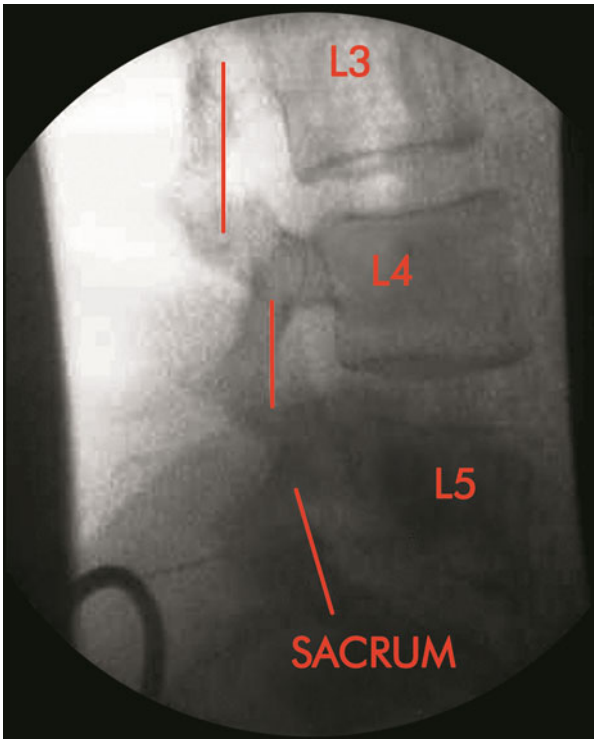

Fig. 3.8 Danger zones!

As you gain experience in the technique, you may decide to slip forward into the groove from the "eye of the Scottie dog" as a matter of routine. After identification of the nerve in the groove means that you are using the shaft of the needle as opposed to its tip, and many workers consider it to be a better way of obtaining a permanent lesion (*see* section on "The Physics of Radiofrequency and Pulsed Radiofrequency").

Once you have achieved localization by sensory stimulation, test for motor stimulation using the following parameters on your machine:

Frequency: 2 Hz
Pulse width: 1 ms
Voltage: double the sensory threshold but at least 1 V

NB it is very common to see localized contractions around the needle area (due to stimulation of the multifidus muscle by the motor component of the medial branch); these can safely be ignored. You are on the lookout for rhythmical contractions in the lower limb. Should these appear, reposition the needle.

You are now ready to carry out a lesion.
Preset the timer to 60 s.
Preset the temperature maximum to 85 °C.
Remove the thermocouple electrode and inject 1 ml of 2 % lidocaine through the needle.
Replace the electrode.

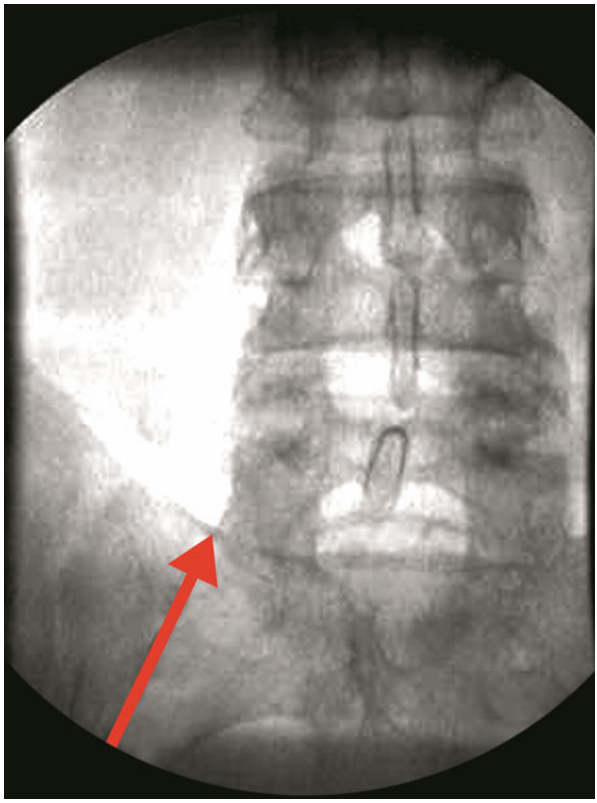

Fig. 3.9 Radiographic landmark on A-P view for L5 medial branch. *Red arrow* indicates the target point for detect L5 medial branch

Switch your machine to *lesion* mode and gradually increase the power, which will in turn cause a temperature rise.

When the temperature reaches 80 °C, switch the timer on, in order to create the lesion. When the lesion has been performed, remove the electrode and inject 1 ml of a mixture of 0.5 % bupivacaine plus a depot steroid preparation in order to reduce postprocedure discomfort.

The Medial Branch of the L5 Posterior Primary Ramus

Your target here is slightly different. With the image intensifier in the posteroanterior axis, visualize the sacrum; your target is the junction between the superior articular process and the upper surface of the lateral part of the sacrum (Fig. 3.9); very often you can locate the medial branch here without needing to move the image intensifier off the posteroanterior axis; instead, you may find it useful to angle your needle, departing from strict "tunnel vision."

Hunt for the nerve as already outlined above.

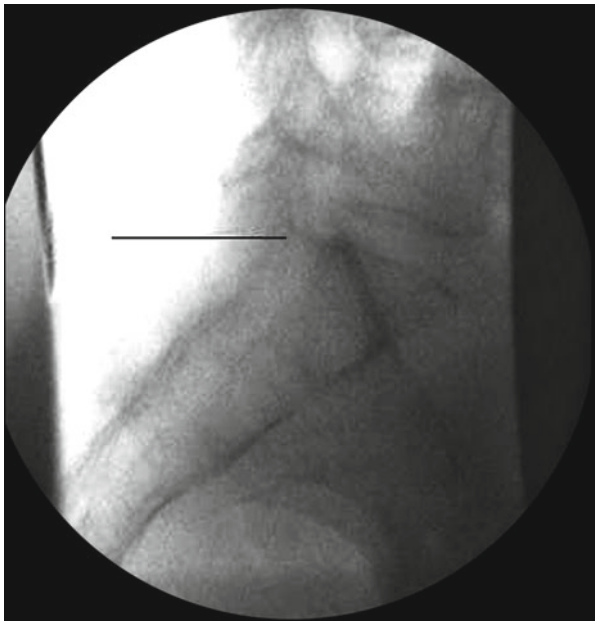

Fig. 3.10 View of needle in lateral axis-2

If you cannot locate the nerve on bone, then slip forward off bone and into the groove close to the intervertebral foramen and try again. If you still cannot locate the nerve, advance deeper *and very slowly* checking the position of your needle in the lateral axis. The tip of your needle must *never* lie anterior to an imaginary line passing through the posterior margin of the L5 intervertebral foramen (Fig. 3.10). If you lesion anterior to this point, you run the double risk of causing neuritis and of damaging the motor root.

As you gain experience in the technique, you may decide to slip forward into the groove from bone as a matter of routine. After identification of the nerve in the groove means that you are using the shaft of the needle as opposed to its tip, and many workers consider it to be a better way of obtaining a permanent lesion (*see* section on "The Physics of Radiofrequency and Pulsed Radiofrequency").

Branch from S1

This lies just lateral to the S1 foramen (Fig. 3.11); you do not need a motor test at this point.

Aftercare

Warn the patient about temporary numbness and limb weakness due to the local anesthetic; do not discharge the patient until you are certain that he/she can walk unaided.

Warn the patient about residual soreness, which may last for a couple of weeks; this usually readily responds to NSAID therapy.

Fig. 3.11 Radiographic landmark for detect the Contribution of S1 to L5/S1 facet joint (*cross mark*)

Evidence

The most recent reviews of the evidence for radiofrequency facet joint denervation are contained in papers written by van Zundert et al. [3] and by Cohen et al. [4].

The technique was given a score of *1B+* (positive recommendation) in a recently published practice guideline for interventional pain management.

The Physics of Radiofrequency and Pulsed Radiofrequency

The following account is reproduced with permission from *Manual of RF Techniques, 3rd. Edition*, by Dr. Charles A. Gauci and published by CoMedical, the Netherlands, 2011.

Section 1

Dr. Eric R. Cosman, Jr., MEng, PhD; Dr. Charles A. Gauci, MD, FRCA, FIPP, FFPMRCA; and Prof. Eric R. Cosman, Sr., PhD

Radiofrequency (RF) lesioning refers to the delivery of high-frequency electrical current in the RF range (≈500 kHz) to patient tissue via an RF electrode to induce a biological effect, such as the thermal destruction of nerves that carry painful impulses. RF methods used in pain management today can be subdivided by the following broad characteristics, each of which involves different physical and clinical considerations.

- *Waveform/Set Temperature*
  - *Thermal RF* (*TRF*): The sustained tissue temperature exceeds 42 °C grossly. A continuous RF (CRF) waveform and tissue temperatures in the range of 70–90 °C are typical. The clinical objective is gross thermal nerve ablation. This category includes "cooled RF" methods, where the electrode is internally cooled, but induced tissue temperatures are neurolytic.
  - *Pulsed RF* (*PRF*): The tissue temperature is held at or below 42 °C on average. RF is delivered in short high-intensity bursts so that the RF electric field strength is increased without gross heating. The clinical objective is neural modification by electric and thermal fields (Cosman and Cosman 2005), but the pain-relief mechanism remains under scientific investigation, as described later on in this book by Cahana et al.
- *Electrode Polarity*
  - *Monopolar RF*: Current passes between a needle electrode and a large-area reference ground pad. RF current intensities are highest near the needle electrode's uninsulated tip. In monopolar thermal RF, an ellipsoidal heat lesion is generated (Fig. 3.12). With proper full adhesion of the ground pad to the skin, current densities are low over the pad's large area, and thus nearby tissue is not typically elevated to lesion levels.
  - *Bipolar RF*: Current passes between two needle-electrode tips, and the current density is high at both locations. Thus, in bipolar thermal RF, a heat lesion is generated near both tips. When parallel tips are brought close together, the electric field is focused between the tips and a large "strip" lesion is formed (Fig. 3.18).

Monopolar thermal RF is the most common and basic form of RF treatment and has been used widely in pain management and neurosurgery since the earliest RF generators were built by B. J. Cosman, S. Aranow, and O. A. Wyss in the early 1950s (Sweet and Mark 1953; Cosman and Cosman 1974, 1984). In the 1990s, monopolar pulsed RF was introduced by Sluijter, Cosman, Rittman, and van Kleef (1998) and is used where conventional thermal RF is contraindicated (e.g., neuropathic pain) or could be potentially hazardous (e.g., DRG lesioning). Bipolar thermal RF between parallel electrodes has been used in pain management for the last decade (Ferrante et al. 2001; Burnham et al. 2007), but only recently has the large size of bipolar RF lesions been fully appreciated (Cosman and Gonzalez 2011). A pioneering application of bipolar pulsed RF has been reported, and this was in the treatment of carpel tunnel syndrome pain (Ruiz-Lopez 2008).

In one author's clinical experience (CAG), there are some basic rules which should be followed in RF lesioning. Thermal RF should be used only for treatment of

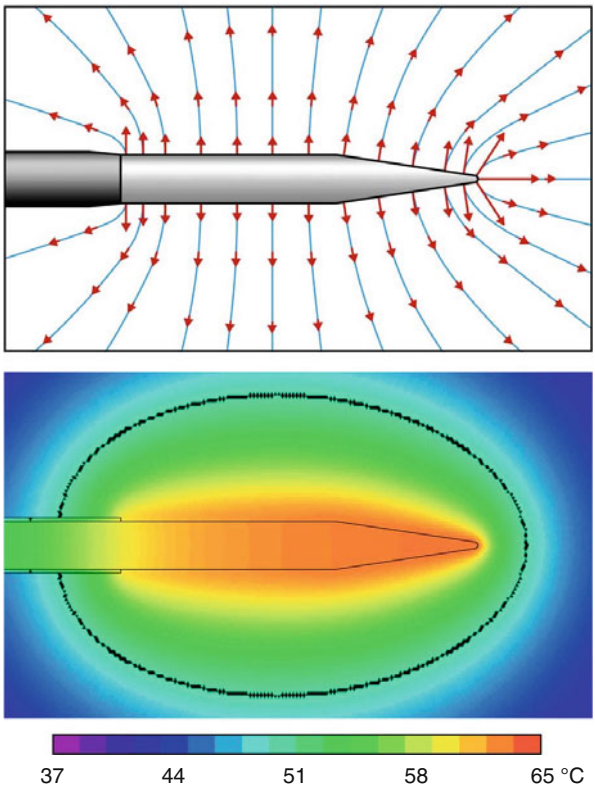

Fig. 3.12 Monopolar thermal RF: electric field (*above*), steady-state tissue temperatures (*below*), and the heat lesion boundary (*black*)

nociceptive pain. RF should not be used in patients with marked psychological overlay and/or drug dependency. RF should not be used in patients with total body pain. You should ensure that the patient has realistic expectations since the total abolition of pain may not be possible. You should exhaust all other nondestructive forms of treatment first and achieve unequivocal benefit from preliminary prognostic blocks.

Monopolar Thermal RF

Using standard equipment, the steps for monopolar RF lesioning in the spine typically include the following steps:

1. Place the ground pad on the skin near the treatment site.
2. Place the RF cannula percutaneously near the target nerve.
3. Stimulate: The RF electrode delivers sensory and motor nerve stimulation to ensure that the cannula's tip is near the target nerve and distant from nontarget nerves.
4. Inject anesthetic through the cannula to prevent pain during lesioning.
5. Lesion: The electrode delivers RF current to the cannula's tip and the nearby nerve(s) are lesioned with temperature control.

The RF cannula is typically a hollow 22G, 21G, 20G, 18G, or 16G needle that is fully insulated except at the tip. The cannula's hollow interior accepts either (a) a stilette to make the cannula solid for insertion, (b) injected fluid anesthetics and steroids, or (c) a 28G thermocouple (TC) electrode for tip temperature measurement and delivery of stimulation and RF currents. In some applications, such as cordotomy, DREZ, brain, and even spinal lesioning, the electrode and cannulae are integrated into a single device. X-ray guidance is typically used to position the cannula nearby the target nerve by reference to bony landmarks. Once positioned, the cannula's stilette is removed and is replaced by the electrode. The operator then seeks the nerve by sensory stimulation, which are low-voltage electrical pulses delivered at 50 Hz (pulses per second). A stronger sensory response at a lower voltage indicates the cannula's tip is closer to the nerve. In the clinical experience of one author (CAG), the cannula needs to be within 3 mm of the nerve in order to create an adequate heat lesion, and a stimulation level of at most 0.6 V is indicative of this.

The operator should always ensure that the cannula/electrode is not dangerously close to any motor nerve in the vicinity of the sensory nerve he/she is trying to lesion. To accomplish this, low-frequency motor stimulation pulses are delivered at 2 Hz. In the clinical experience of one author (CAG), if no muscle twitch in the territory of the nerve is noted at twice the voltage strength necessary to achieve sensory stimulation, it can be safely assumed that there are no motor paths within 3 mm of the needle and that, consequently, there is no risk of damage to any motor nerve. When working on spinal nerves, e.g., medial branches of posterior primary rami, one should not worry about localized contractions close to the area of needle insertion; one is concerned with motor twitches at more distant sites, e.g., the arm or the leg.

When the operator is satisfied that the needle is safely in position, RF current is delivered to the electrode and cannula. Frictional heating occurs near the cannula's uninsulated tip due to tissue electrolytes being pulled to and fro by the RF current alternating at approximately 500 kHz (500,000 cycles per second). While heating occurs only in the tissue and not within the electrode, within a few seconds of sustained RF heating, the temperature measured in the electrode/cannula's tip registers the maximum tissue temperature (Cosman and Cosman 2003; Cosman 2010) (Fig. 3.12). This occurs due to coherent heat diffusion into the electrode tip from all sides. This maximum temperature can be directly controlled by the operator. It must be cautioned that for cooled RF, where the electrode is cooled by internally circulating water, the electrode does not measure the maximum tissue temperature; rather, the maximum tissue temperature occurs at a variable location remote of the electrode and can far exceed the temperature measured within or nearby the electrode (Wright 2007). As the current is applied at the destructive levels typical of thermal RF, a well-circumscribed heat lesion appears. It will grow until a steady state is reached; at this point, the passage of current only maintains the temperature. Little further spread takes place at the edge of the lesion, since (a) the electric field and rate of heating decrease with distance from the electrode and (b) the rate of RF heating within the lesion volume is roughly balanced by the rate of heat diffusion into the surrounding tissue, heat diffusion into the electrode shaft, and blood-flow cooling.

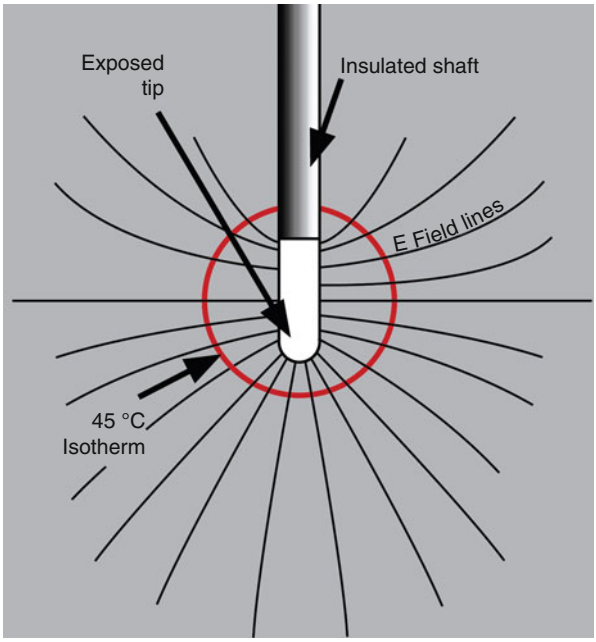

Fig. 3.13 Monopolar thermal RF lesion zone and the 45 °C isotherm (Adapted from Cosman and Cosman (1984))

The heat lesion is shaped like a match head (Fig. 3.12) and is commonly defined as the tissue regions for which the temperature exceeds 45–50 °C for at least 20 s (Brodkey 1964; Dieckmann 1965; Smith 1981; Cosman and Cosman 1974, 1984). Though permanent neurological damage occurs when tissue is exposed to temperatures exceeding 42 °C over longer durations (Cosman et al. 2009), for practical purposes, when we talk about lesion size, we mean the volume of tissue within the 45 °C isotherm (Fig. 3.13). According to Abou-Sherif et al. (2003), thermal RF produces the following effects in the rat sciatic nerve at 6–8 weeks: Wallerian degeneration in all nerve fibers, physical disruption of the basal laminae, focal disruption of the perineurium, degranulation of mast cells, recruitment of exogenous macrophages, local muscle necrosis, delayed axonal regeneration, and prolonged changes in the microvascular bed (vascular stasis) with extravasation of erythrocytes, this latter resembling the ischemic changes of reperfusion injury.

The heat lesion extends maximally around the shaft of the cannula, with a diameter that ranges from 2 to 10 mm depending on the cannula's diameter/gauge, the tip temperature, and lesion time (Fig. 3.14). The lesion extends 1–2 mm both ahead of the tip and up the shaft, yielding a total length 2–3 mm longer than the tip length (Cosman and Cosman 1984). Because of this geometry, many physicians prefer "parallel"/"side-on" cannula placement for monopolar thermal RF lesioning so that the nerve is positioned at the side of the cannula tip where the lesion extends maximally. In the alternative "perpendicular"/"point-on" approach, the nerve is placed directly ahead of the cannula tip, thus exposing a smaller volume of the nerve to neurolytic temperatures.

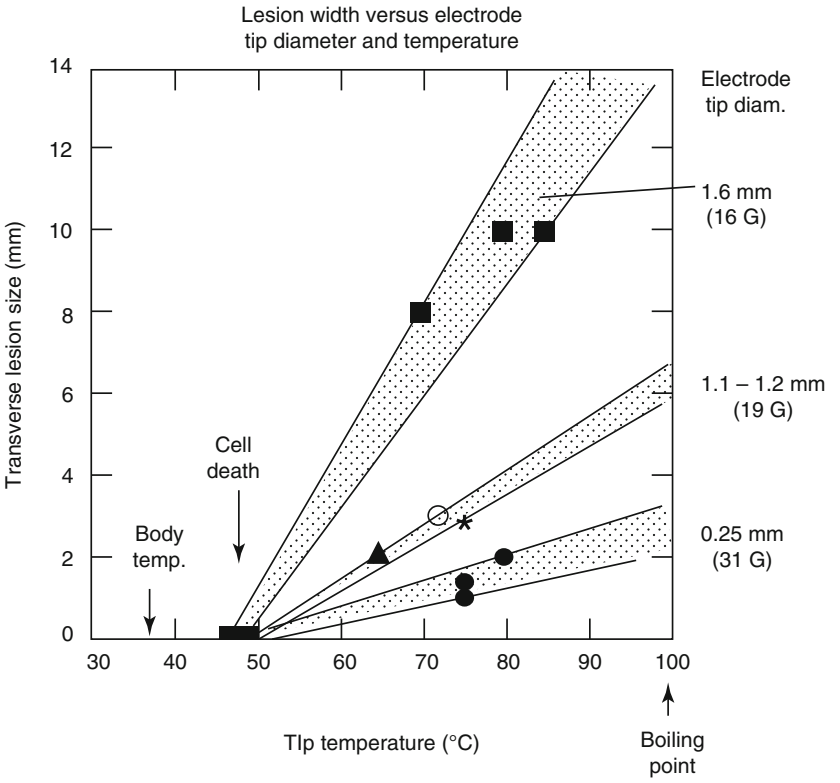

Fig. 3.14 Postmortem monopolar thermal RF lesion width around the electrode shaft for different electrode diameters/gauges and tip temperatures (Adapted from Cosman et al. (1988))

For a given electrode/cannula tip temperature, if lesion size is plotted against exposure time, it will be observed that the size increase is relatively linear over the early part of the curve, but then begins to slow as the steady state is approached (Fig. 3.15). For electrode/cannula of the sizes used in pain management, the steady-state lesion size is not reached until 30–90 s after the tip temperature reaches its set value. Thus, the tip should be held at the desired temperature for this duration of time to ensure that the lesion has reached its full spread for that temperature. The steady-state lesion size (Fig. 3.16) is strongly influenced by the tip temperature and electrode/cannula diameter (Fig. 3.14). All other things being equal, a larger heat lesion will be produced by a larger electrode tip and a higher tip temperature (assuming that boiling does not shut down RF current flow). Additionally, several factors can affect lesion size and dynamics, including variations in tissue densities, proximity to bone, and proximity to CSF (especially in trigeminal lesions), blood vessels, etc.

It is advisable to keep the tissue temperature below boiling (100 °C). Boiling can lead to uncontrolled gas discharges, burning steam that travels up the electrode's shaft to the skin, irregular lesion geometry, and charring at the electrode tip. In one

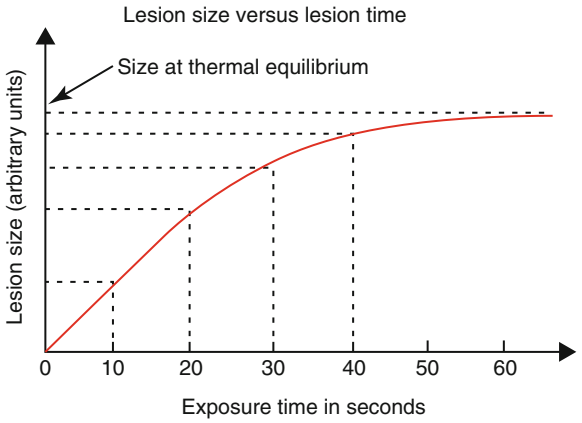

Fig. 3.15 Schematic plot of thermal RF lesion size vs. exposure time to RF current (Adapted from Cosman and Cosman (1974))

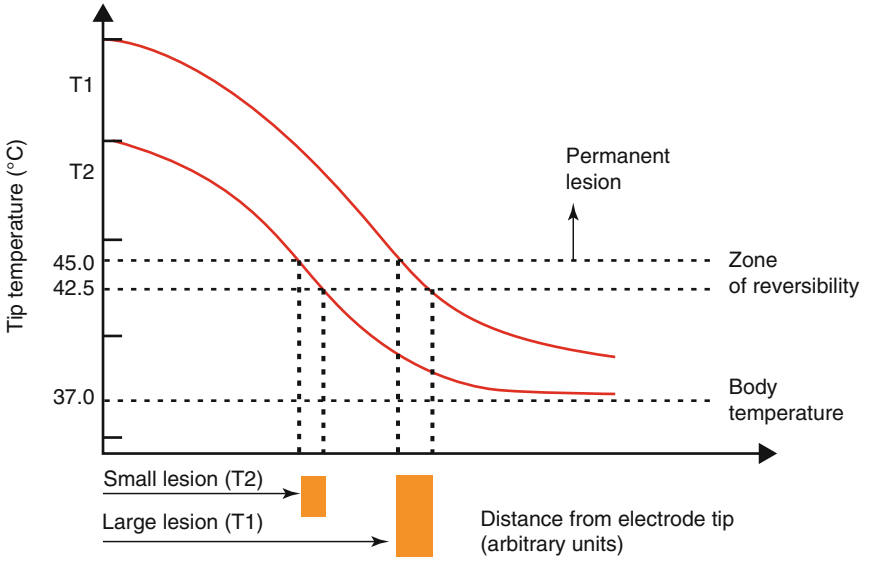

Fig. 3.16 Effect of tip temperature on RF lesion size (Adapted from Cosman and Cosman (1974))

author's clinical practice (CAG), the lesion temperature is held below 85 °C to give a broad temperature margin relative to 100 °C.

The resistance to the flow of electrical current from the tip of the cannula, the impedance, can be measured and should be observed by the operator. A very high impedance, or open circuit, can indicate that the electrode or ground pad is not in proper contact with the patient or that the cables are disconnected. A rising, high impedance can also indicate that the tissue is boiling at the cannula's tip, since electrical current cannot easily traverse boiling gas bubble; this is an important safety check in case the temperature sensor is broken or misplaced outside the cannula's tip (Cosman 2010). A very low impedance, or short circuit, can indicate a failure of the RF equipment or direct contact between the electrode and the ground pad or

Fig. 3.17 RF Generators (**a**) The Cosman G4 four-electrode RF generator (**b**) NeuroTherm NT2000 RF lesion generator (**c**) Kimberly-Clark Pain Management System (**d**) Diros OWL URF-3AP Multi-Lesion

contact with a large metallic implant. Impedance can also be of use in certain procedures since it can indicate the tissue type in which the cannula's tip is positioned. For example, during a percutaneous cordotomy, the impedance will be 400 Ω when the tip is in the extradural tissues, fall to 200 Ω as the needle tip enters the CSF, and then rise to over 800 Ω as the needle tip enters the spinal cord. When working in the intervertebral disc, the impedance is usually very high in the outer annulus, falling to less than 200 Ω in the nucleus pulposus.

For facet denervations, some physicians use "pole needles." These are non-temperature-monitoring, tissue-piercing electrodes with integrated, flexible, fluid injection lines. They are used when it is felt that the electrode position must not be perturbed through stimulation, injection, and lesioning. Typically, 20 V is applied with the expectation of producing an 80 °C heat lesion. However, in vivo clinical experiment shows that the tip temperature is not consistently 80 °C but rather can range from values less than 80 °C to those exceeding boiling (Buijs et al. 2004; Gultuna et al. 2011). As such, when pole needles are used, one should halt RF delivery if an impedance rise is observed that indicates tissue boiling; and when precise lesion control is required, one should use temperature-monitoring injection electrodes.

Four standard radiofrequency lesion generators in common use around the world are shown in Fig. 3.17.

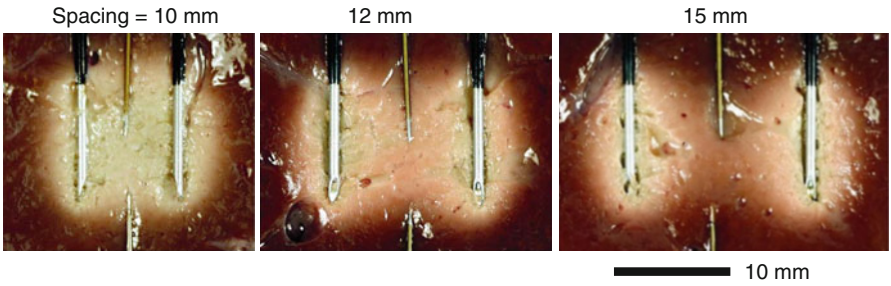

Fig. 3.18 Bipolar lesion size for 20 gauge, 10 mm tip length, 90 °C, 3 min, and increasing spacing: strip $12 \times 15 \times 8$ mm^3 (*left*), strip $10 \times 17 \times 5$ mm^3 (*middle*), and two Ellipsoids $12 \times 7 \times 7$ mm^3 (*right*)

Bipolar Thermal RF

Whereas a monopolar configuration drives RF current between an electrode's exposed tip and a distant ground pad, a bipolar configuration drives RF current between two nearby electrode tips. As bipolar electrode tips are brought closer together, the resulting thermal lesion shape transitions from that of two volumes surrounding each tip separately to that of a single volume connecting the tips (Fig. 3.18). The connected geometry and larger total lesion volume are strongly influenced by a focusing of the electric and current density fields between closely spaced electrode tips. Bipolar electrodes can be arranged collinearly or in parallel, but parallel arrangements produce the largest lesion size increases (Cosman et al. 1984). Important features of parallel bipolar heat lesions include:

- *Large*: Bipolar RF lesions are larger than cooled RF lesions as used in pain management (Figs. 3.19 and 3.20, *left*). The size of one bipolar RF lesion is roughly that of three conventional monopolar RF lesions placed side by side (Fig. 3.20, *right*).
- *Conformal*: Bipolar RF applied to closely spaced electrode tips produces heat lesions shaped like a rounded brick, also known as a "strip lesion." To conform to anatomical constraints, the width and length of the strip can be adjusted nearly independently of each other and the lesion depth (Fig. 3.18). As such, a large lesion can be produced without unnecessary damage to healthy tissue and with reduced risk to sensitive structures. This is not possible for monopolar lesions around a cylindrical electrode since the lesion width and depth are the same.
- *Connected strip lesions*: By leapfrogging electrodes (Ferrante et al. 2001), brick-like strip lesions can be placed side by side without gaps to produce an elongated lesion zone that has consistent height and thickness (Figs. 3.20, *middle*; 3.21). This is not possible for cooled and conventional monopolar RF without positioning electrodes very close together.
- *Robust*: Strip lesions can be generated reliably for parallel tip spacings of 10 mm, tip temperature 90 °C, and lesion time 3 min. Perturbations of these geometric and RF parameters do not substantially affect lesion size (Cosman and Gonzalez

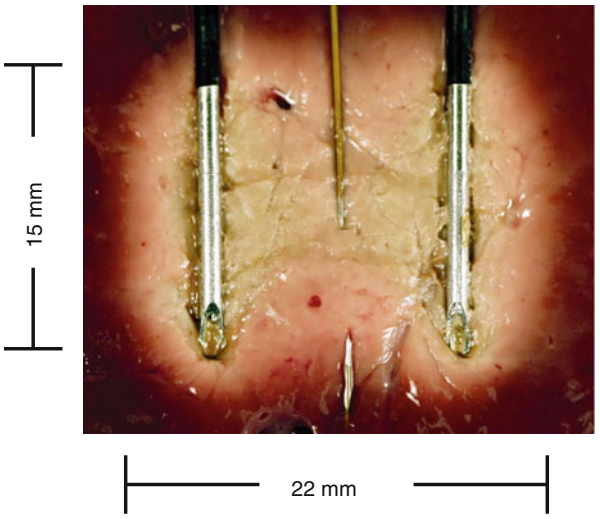

Fig. 3.19 Bipolar heat lesion size is 15 × 22 × 8 mm^3 for 18 gauge, 15 mm tip length, 15 mm spacing, 90 °C, 3 min

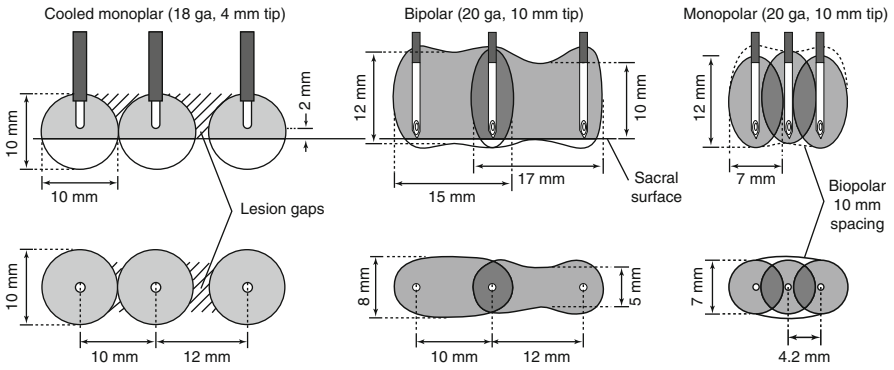

Fig. 3.20 Comparison of bipolar RF lesion size with that of cooled and conventional monopolar RF

2011; Fig. 3.18). The tip temperature and lesion time used for bipolar RF are greater than those used for monopolar RF since it is desired that larger heat lesions are formed.

As an example, all these features are illustrated by the RF palisade approach to sacroiliac joint (SIJ) denervation (Fig. 3.21). In this approach, four to five large bipolar RF lesions are placed side by side like bricks in wall to traverse the region between the dorsal sacral foramina and SIJ line in which sacral lateral branch nerves form the SIJ's dorsal innervation. While each lesion is large in the inferior-superior direction, its depth is constrained in the left-right direction, thus reducing the risk of damage to the sacral nerve roots. Because lesion size is robust to variations in tip spacing and because adjacent lesions overlap, the total lesion zone has a consistent thickness and height from the sacral surface.

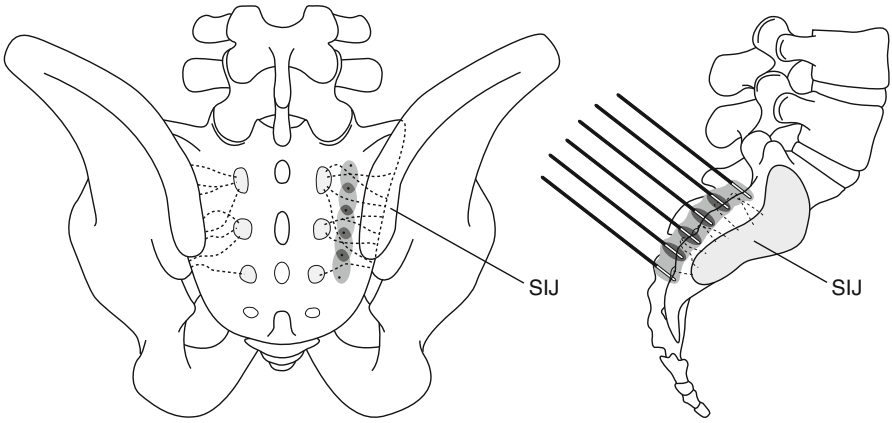

Fig. 3.21 Palisade sacroiliac joint denervation

Bipolar RF lesions of the sizes shown in Fig. 3.18 have been used successfully in pain management (Ferrante et al. 2001; Burnham et al. 2007; Cosman and Gonzalez 2011). Ex vivo experiments by Cosman and Gonzalez (2011) document further flexibility in the size and shape of bipolar lesions. Indeed, bipolar lesions with dimensions exceeding 2 cm can be readily created with standard RF equipment. As for all RF lesioning, before the clinical use of novel bipolar configurations, a physician must consult lesion-size studies to determine whether that configuration is appropriate for the target anatomy. The proximity of target nerves to nontarget nerves, blood vessels, skin surface, and other sensitive structures imposes an upper bound on the safe size of any heat lesion, especially in the spine.

Monopolar Pulsed RF

While making a radiofrequency lesion in the standard thermal RF mode, the tissue which surrounds the tip of the electrode is exposed to a concentrated electric field that induces tissue heating (Fig. 3.12). The electric field (E-field) intensity decreases precipitously with distance from the tip, falling to a low level at distances beyond the extent of a typical heat lesion (Cosman and Cosman 2005). Since the high temperatures within the heat lesion volume reliably induce cellular death, it is assumed that the E-field per se has little or no clinical effect in thermal RF.

The introduction of pulsed RF (Sluijter et al. 1998) was motivated by the desire to expose nerves to high electric fields without gross neurodestructive heating, so as to reduce the risk of RF treatment in sensitive anatomy such as the DRG. In the mid-1990s, Cosman and Sluijter modified a standard lesion generator to deliver radiofrequency voltage bursts at a repetition rate of 2 Hz. Since each burst is only 20 ms long, the intervening inactive period 480 ms allows heat to dissipate into the surrounding tissue after exposure to the electric field (Figs. 3.22 and 3.23). As such, the

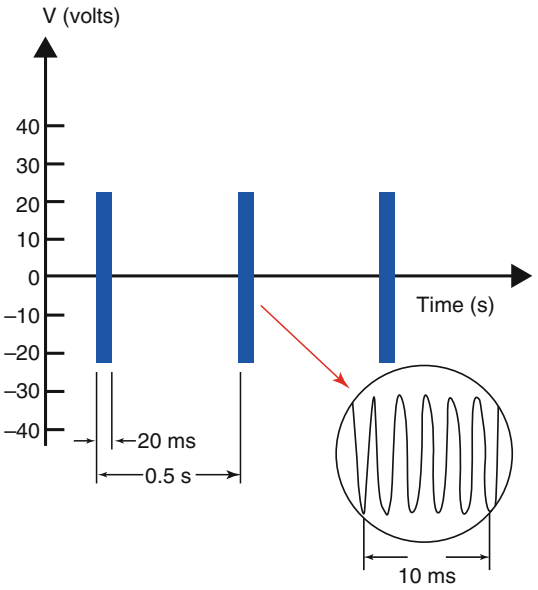

Fig. 3.22 Pulsed RF. *Red arrow* indicates the target point for detect L5 medial branch.

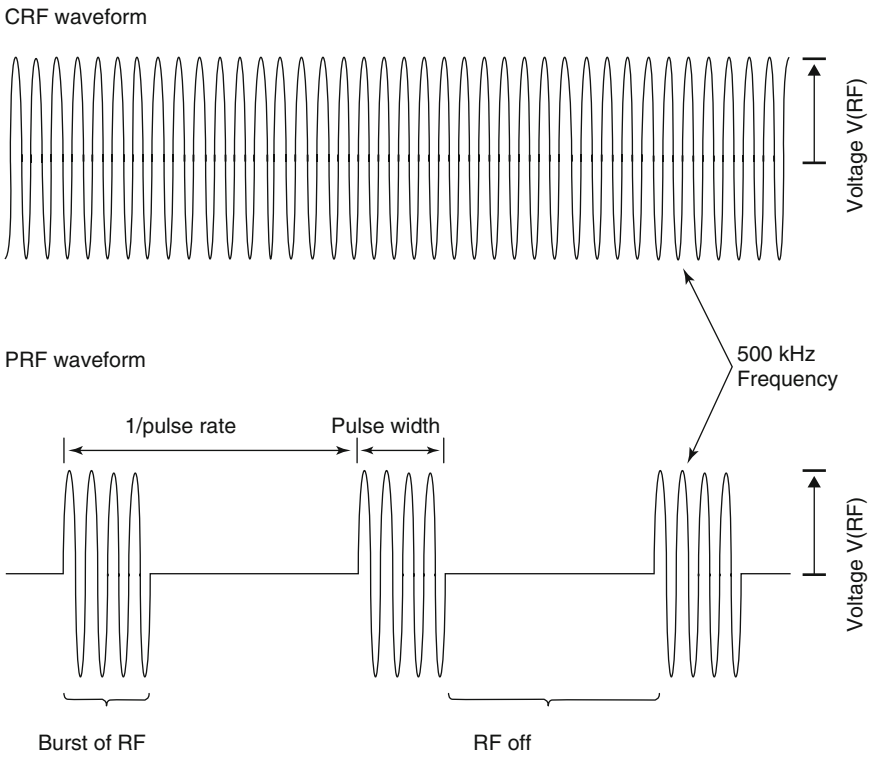

Fig. 3.23 Schematic RF waveforms for CRF and PRF (parameters and times not to scale)

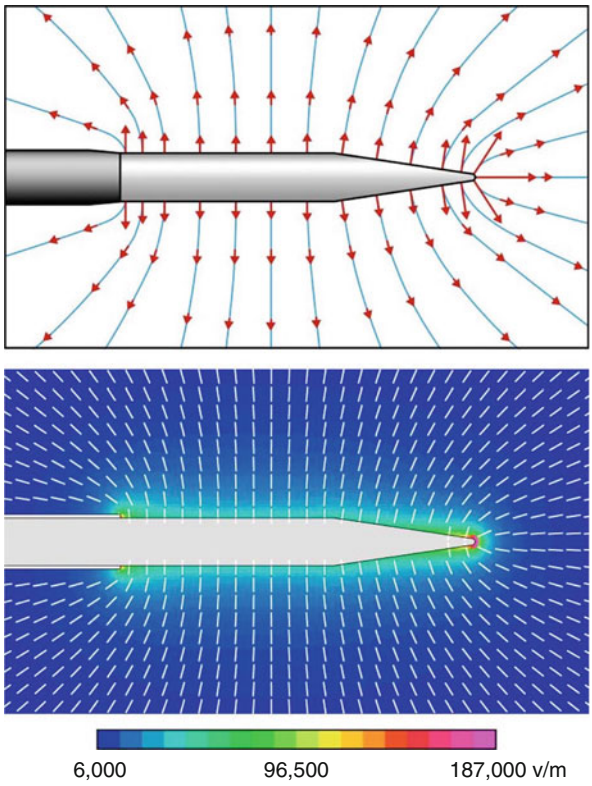

Fig. 3.24 (*Top*) schematic E-field patterns. (*Bottom*) E calculated in tissue for a 22~ electrode at V(RF) = 45 V

RF voltage, and thus the E-field strength, can be increased while holding the electrode tip temperature at or below 42 °C, a level assumed not to produce gross neurodestructive effects (Fig. 3.24). Cosman and Cosman (2005) have shown that tissue around the electrode shaft is broadly exposed to high-intensity E-fields without substantial heating. They also showed that the very intense electric fields at electrode's pointed tip cause "hot flashes" during each RF burst. The full details of this physical geometry is given later on in this book, but some salient points are:

- Ahead of the tip: Within ≈0.2 mm of the electrode point, temperature spikes into the neurolytic range and above the measured tip temperature during each burst of RF (Fig. 3.25). At larger distances and between RF bursts, the temperature does not substantially exceed that of the electrode tip. While the electric field is maximal within ≈ 0.2 mm of the electrode point, it falls off very quickly with distance ahead of the tip so that beyond ≈0.2 mm, its magnitude is smaller ahead of the tip than it is lateral to the shaft (Fig. 3.26).
- Around the shaft: Temperature does not substantially exceed the measured tip temperature. The electric field falls off slowly with distance and exposes tissue to electrical forces that are high in biological terms and that appear to produce a

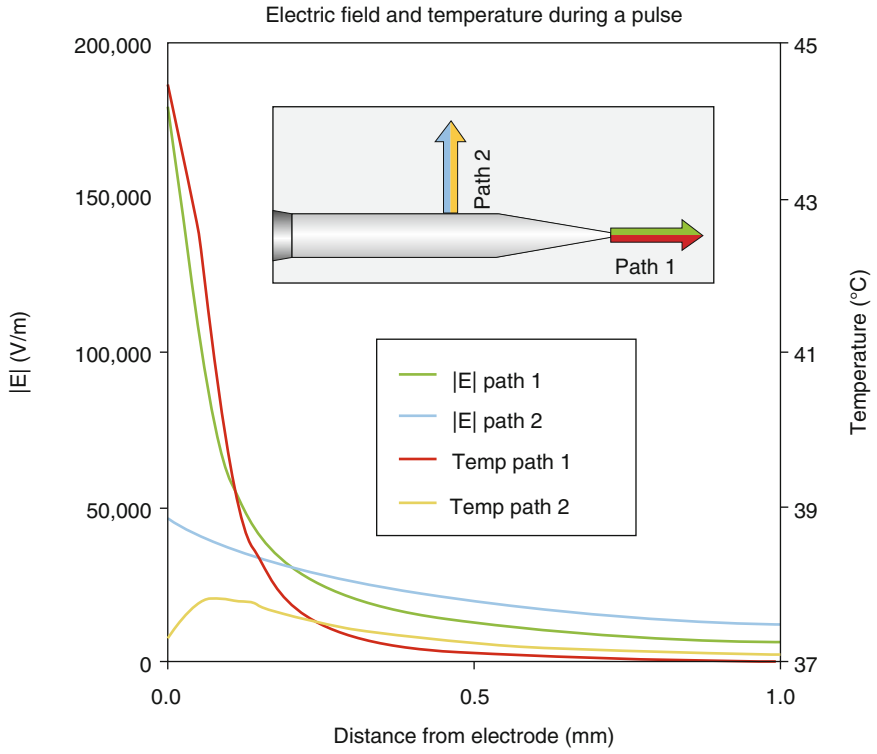

Fig. 3.25 E-smd T-fields during the first PRF pulse for V(RF) = 45 V and pulse width = 20 ms

disruptive effect (Erdine et al. 2009); as such, its range of influence is broader around the shaft than ahead of the tip (Figs. 3.26 and 3.27).

In typical pulsed RF practice, the generator is set to target pulse voltage = 45 V, pulse width = 20 ms, and pulse rate = 2 Hz. The generator then automatically adjusts the either the pulse voltage, the pulse width, or less commonly the pulse rate to maintain the temperature at or below 42 °C for 120 s. Sluijter (personal communication, 1998) further recommends that the tissue impedance be reduced by the injection of about 1 ml of local anesthetic or normal saline. This is an approach supported by finite-element calculations of the electric field that assume directional saline spread toward the nerve (Cosman and Cosman 2005a). Dr. Bill Cohen (personal communication, 1998) also advocates saline injection and has observed the spread of fluid injection toward the nerve using X-ray contrast.

The clinical effects and pain-relief mechanism of pulsed RF is the subject of ongoing scientific investigation. Though there is growing evidence that pulsed RF has a physical effect on nerves (see Cahana et al. later on in this book), in the absence of an established model of PRF's pain-relief mechanism, what is known about pulsed RF's pain-relief efficacy depends on clinical trials using specific

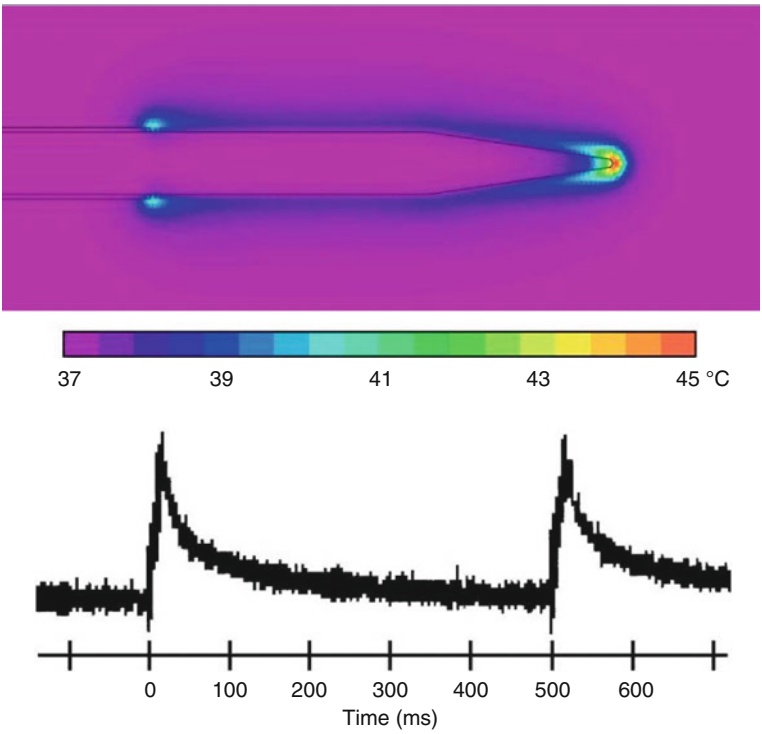

Fig. 3.26 Hot flashes during a PRF pulse

parameters and control algorithms. Since the first publication about the clinical use of pulsed RF in pain management, numerous peer-reviewed clinical studies of pulsed RF technique and pain-relief outcomes have been published, including an RCT related to PRF treatment of cervical radicular pain (Van Zundert et al. 2007). While treatment parameters vary somewhat, these published clinical trials generally use set values voltage = 45 V, pulse width = 20 ms, pulse rate = 2 Hz, and treatment time = 120 s, and they all use delivery algorithms that vary either the pulse voltage or the pulse width to maintain the temperature at or below 42 °C. Beyond this, a number of questions about pulsed RF methodology remain unanswered:

Is it better to approach a nerve "side-on" or "point-on" with a PRF electrode?

Many clinicians prefer to use the point-on/perpendicular approach as they feel this allow for more precise targeting, with greater electric field effect. While this may be valid, since the E-field is very large only within a very small distance ahead of the electrode point (≈0.2 mm), and otherwise falls to intensities less than those around the electrode shaft, it is unlikely that the very large E-field at the electrode point accounts for the full clinical effect. Further, since the E-field at the point has destructive intensity and is coincident with high-temperature hot flashes, the point-on approach cannot be having a purely nondestructive effect. On the other hand, since the E-field intensity

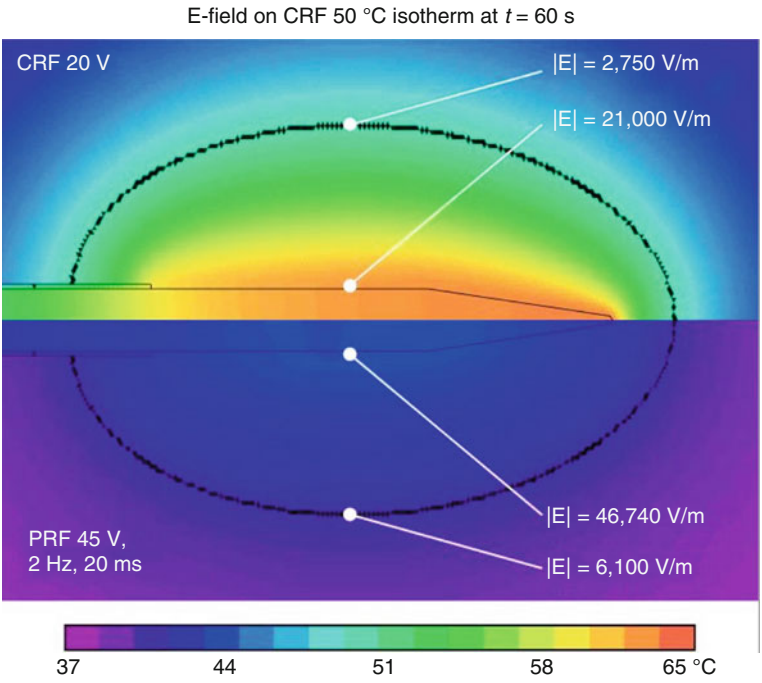

Fig. 3.27 E-fields dominate over T-fields in PRF. The opposite is true for CRF

declines less precipitously lateral to the electrode shaft, the side-on/parallel approach exposes a larger nerve volume to elevated electric fields, with less heating. Recent animal studies by Erdine et al. (2009) show that the side-on approach can disrupt axonal microtubules, microfilaments, and mitochondria. Clinical trials are required to determine the relative efficacy of the side-on and point-on methods.

Can clinical outcomes be improved by changing the typical set values?

Voltage = 45 V, pulse width = 20 ms, pulse rate = 2 Hz, and treatment time = 120 s? These parameters were selected for practical purposes by PRF's inventors, and there is no clinical evidence that they are "ideal" in any sense. Many workers use longer treatment times in excess of 4 min, or pulse width = 10 ms and pulse rate = 4 Hz, as they feel it augments the electric field exposure, also known as E-dose (Cosman and Cosman 2005). While these variations may prove useful, there is currently no clinical proof that any such variations improve outcomes.

Do clinical outcome vary depending on the temperature control algorithm?

Modern RF generators (Fig. 3.17) implicitly incorporate at least one method of PRF temperature control that varies either pulse voltage, pulse width, or pulse rate, while fixing the other parameters. For example, the NeuroTherm NT 1100 generator's promotional literature refers to its particular pulse-rate algorithm by the trade name pulse dose. The Cosman G4 generator incorporates an E-dose setting that allows the operator to select between control algorithms to adjust a nerve's exposure

to the E-field. While all clinical studies showing positive PRF outcomes to date employ generators that vary either the voltage or the pulse width to control temperature, they do not compare these control methods. The authors are not aware of any clinical study of PRF outcomes in which temperature is controlled by varying the pulse rate or using pulse dose. There is theoretical reason to believe that pulse-rate/pulse-dose algorithms may be less effective if PRF's mechanism depends on long-term depression (LTD). The LTD hypothesis of PRF pain relief was proposed by Cosman and Cosman (2005) and is based on the idea that PRF stimulates action potentials and thus subthreshold postsynaptic potentials at 2 Hz, which falls within a rate range known to induce LTD using conditioning stimulation (Sandkuler 1997; Bear 2003). Since a pulse-rate/pulse-dose algorithm may reduce the pulse rate substantially below the known LTD range, it may also reduce the LTD effect. Voltage and pulse-width control algorithms do not suffer from this concern. Nevertheless, in the absence of strong model of PRF's mode of action or clinical trials, PRF temperature control algorithms cannot be clinically distinguished.

Section 2

Dr. Eric R. Cosman, Jr., MEng, PhD and Prof. Eric R. Cosman, Sr., PhD

There are two output modes of RF generators that are used today to produce pain relief. The first is the standard, thermal RF mode which uses a continuous sinusoidal waveform RF output, commonly referred to as continuous RF or CRF. The second uses a series of pulsed bursts of RF signal, referred to as pulsed RF or PRF. The amplitude, V(RF), of both these waveforms is measured in units of voltage (*V*). For voltages commonly used in clinical practice, a continuous RF waveform produces a heat lesion. This means that the neural tissue near the uninsulated, metal electrode tip is heated continuously to destructive temperatures (greater than 45–50 °C) by ionic friction of the RF currents in the tissue. Thus, the CRF lesion volume includes all tissue within the 45–50 °C isotherm boundary, which tends to have an ellipsoidal shape that encompasses the electrode tip. Within this lesion volume, all cell structures are macroscopically destroyed by heat. The action of pulsed RF on neural tissue is different. Because the RF output is delivered in bursts of short duration relative to the intervening quiescent periods, the average temperature of the tissue near the electrode is not raised continuously or as high as for continuous RF at the same RF voltage. Since the PRF voltage is typically regulated to keep the average tip temperature in a nondestructive range, other mechanisms produce the clinically observed pain-relieving effects.

The electric field, E, is the fundamental physical quantity that governs all the actions of RF output on neural tissue, both for pulsed RF and for continuous RF modes. The electric field is created in space around an RF electrode that is connected to the output voltage V(RF) from an RF generator (Fig. 3.13). E is represented by an arrow (vector) at every point in space around the electrode tip, indicative of the magnitude and the direction the force it will produce on charged structures

and ions in the tissue. The E-lines indicate the pattern of E in a homogeneous medium. The E-field produces various effects on tissue including oscillations of charges, ionic currents, charge polarizations, membrane voltages, and structure-modifying forces. For continuous RF mode, the dominant consequence of these effects is the production of heat in the tissue caused by frictional energy loss due to the ionic currents that are driven by the E-field. However, for pulsed RF, the effects of E-field are more complex and varied and range from heat flashes, to modification of neuron ultrastructure, to neural excitation phenomena. All of these effects can play a role in neuronal modification, though exactly how they produce antinociception in PRF treatments is an area of active scientific investigation.

To understand any of the E-field effects of pulsed RF, the magnitude of the E-field around an actual electrode in tissue must be determined. This has been calculated for a typical electrode during a PRF pulse (Figs. 3.13, 3.23, and 3.25) using finite-element computational methods (Cosman and Cosman). The quantitative values of E and temperature T at distances from the electrode tip are plotted in (Fig. 7c) for a 22 Ga electrode at V(RF) = 45 V. Near the sharp point of the electrode, the E-field has strength of up to 187,000 V/m. This drops off rapidly with distance from the point. At the side of the electrode, E is 46,740 V/m and drops off more slowly with lateral distance. These are very high E-fields in biological terms and are capable of a variety of modifications of neurons that account for the effects of pulsed RF.

Two consequences of these predictions are supported by experimental and clinical observations. The first is that, as a consequence of the very high E-fields at the electrode tip, there are hot flashes at the electrode tip that can be thermally destructive to neurons. The second is that there are significant nonthermal effects of the E-field on neurons at positions away from the point of the tip that are certainly related to the pain-relieving effects of PRF.

During the brief RF pulse, a hot spot occurs at the tip which can be 15–20 °C above the average tissue temperature of the tissue that remains near body temperature of 37–42 °C. This has been confirmed by ex vivo measurements and finite-element calculations. The intense E-field and hot flashes could be expected to have destructive effects on neural tissue very near the tip point. Evidence for such destruction has been observed in vitro (Cahana et al.). This may play a role in PRF's clinical effect when electrode point is in the nerve or pressing against the nerve. However, it is unlikely that such focal effects can account for all of PRF pain relief, since the region of extremely high E-fields and T hot flashes are likely confined to less than about 0.2 mm radius from the electrode point.

There is evidence that direct, nonthermal effects are important in PRF. It is known that pain relief can be achieved when the side of the electrode tip, not the tip point, is next to an axon or DRG. While the hot flash fluctuations are less than 1 °C at 0.5 mm from the tip in any direction for typical PRF voltages, at lateral distances of greater than 1 mm, the magnitude of the electric field is still large in biological terms. For example, finite-element computation of the E-field for V(RF) = 45 V predict that the E is 20,000 V/m at 0.5 mm and 12,000 V/m at 1.0 mm laterally. Thus, neuronal modifications in this E-field range should be significant.

Comparison of E and T strengths between typical CRF and PRF waveforms shows striking differences between these RF modes (Fig. 7e). Calculations predict that after 60 s of CRF at V(RF) = 20 V, E = 21,000 V/m and T = 60–65 °C at the lateral tip surface and E = 2,750 V/m and T = 50 °C at 1.8 mm away. In contrast, after 60 s of PRF with V(RF) = 45 V, E = 46,740 V/m and T = 42 °C at the lateral tip surface and E = 6,100 V/m and T = 38 °C at 1.8 mm away. In other words, in PRF, the direct electric field effects are more prominent, whereas in CRF, the thermal fields are more prominent and largely mask the E-field effects.

Combined with the understanding that PRF has a clinical effect even when the electrode is not placed on the nerve directly, these physical observations suggest that the E-field is directly involved in the analgesic effect of PRF. It is known that PRF E-fields produce significant transmembrane potentials on the neuron membrane and organelles (Cosman and Cosman 2005). The E-field can also penetrate the membranes of axon and the DRG soma to disrupt essential cellular substructures and functions. For example, PRF applied to the DRG of rabbits causes pronounced neuron ultrastructural modifications that are seen only under electron microscopy (Erdine et al. 2005) and that are likely to modify or disable the cell's function. Additionally, PRF applied to afferent axons in the rat sciatic nerve with a "parallel"/"side-on" approach causes disruption of microtubules, microfilaments, and mitochondria; the disruption appears to be more pronounced in C fibers than in A-delta and A-beta fibers (Erdine et al. 2009). This would suggest that PRF can produce subcellular, microscopic lesions on neurons in a volume around the electrode, possibly resulting in reduction of afferent pain signals. Blockage of axonal transmission of action potentials has been observed in the sural and sciatic nerves of rats using electrophysiological microelectrode recording on individual teased nerve fibers (Cosman et al. 2009); the blockage occurs at lower voltages for a "perpendicular"/"point-on" approach than it does for a "parallel"/"side-on" approach, likely due to the very high E-field and hot flashes present at the electrode's pointed tip. PRF membrane potentials are also capable of neural excitations (action potentials) by a process called membrane rectification. This excitation has been observed in the sural and sciatic nerves of rats using the aforementioned teased-fiber recording technique (Cosman et al. 2009). Because the PRF pulse rate is similar to that of classical conditioning stimulation (1–2 Hz), it has been proposed that PRF may have a similar action (Cosman and Cosman 2005). Conditioning stimulation is capable of suppressing synaptic efficiency of A-delta and C-fiber afferent nociception signals (Sandkuhler), a phenomenon known as long-term depression (LTD). Therefore, the PRF might be reducing transmission of pain information by LTD of synaptic connections in the dorsal horn. The appropriate exposure of PRF for a given pain syndrome and anatomical target, for either microscopic or LTD mechanisms, should be governed by the PRF "E-dose" (Cosman and Cosman 2005). E-dose provides a parametric measure of E-field strength and integral pulse/time exposure.

Section 3

Prof. A. Cahana, MD, DAAPM, FIPP; Prof. Philippe Richebé, MD, PhD; and Dr Cyril Rivat, PhD

Cosman and Cosman (2005) have shown that pulsed RF (PRF) exposes tissue to higher electric field (E-field) intensities than does continuous/thermal RF (CRF), as illustrated in Fig. 7e. For a CRF heat lesion with tip temperature 65 °C, the E-field strength is 21,000 V/m around the needle, as compared to 46,740 V/m for a PRF lesion with tip temperature 42 °C. At a lateral distance from the shaft roughly coincident with the outer limit of the CRF heat lesion, the CRF E-field strength is 2,700 V/m, whereas the PRF E-field strength is 6,100 V/m. Furthermore, since PRF produces lower temperatures around the shaft, the tissue that would be exposed to neurolytic temperatures in the CRF case is principally exposed to high E-fields in the PRF case. As described earlier, the E-field strength is highest within ≈0.2 mm of the pointed needle tip; transient, focal, high-temperature spikes are also present during each RF pulse at this location. On the other hand, since the E-field intensity decreases less precipitously around the shaft than ahead of the tip, it has a higher intensity over a larger range around the shaft than it does directly ahead of the tip.

In the light of all the recent work on pulsed radiofrequency, many workers prefer to use the needle tip ("perpendicular approach") as they feel that this approach allows for more precise targeting. They feel that use of the needle tip combines a reduced heat effect with a greater electric force effect and therefore carries with it a theoretically reduced risk of neuritis than would use of the needle shaft. There is, however, no scientific evidence for this hypothesis!

Sluijter describes four phases in a pulsed radiofrequency procedure, viz.:

- A stunning phase, which provides immediate relief.
- A phase of postprocedure discomfort, which may last for up to 3 weeks.
- A phase of beneficial clinical effect, which is of variable duration.
- A phase of recurrence of pain; we are still in the early days but many cases record 4–24 months of relief.

There is no clinical evidence of any nerve damage with pulsed radiofrequency. Higuchi et al. (2002) have presented experimental evidence that pulsed radiofrequency applied to the rat cervical dorsal root ganglion causes upregulation of the immediate early gene c-fos [4].

With the technological improvements made during the last decade, cellular and ultrastructural effects of PRF and RF have been better evaluated.

Pulsed radiofrequency does seem to have a clinical effect on peripheral nerves. Hamann (2003) pointing out the lack of laboratory evidence for this phenomenon felt that this may be due to changes induced in the function of the Schwann cells [5]. Cahana et al. (2003) have shown that pulsed radiofrequency affects cell cultures only within a range of 1 mm, raising questions as to how close to the target tissue one needs to be with the electrode [6].

Podhajsky et al. (2005) compared histologic effects of CRF, PRF, and continuous heat at 42 °C on DRG and sciatic nerves 2, 7, and 21 days after procedure. PRF did not induce any paralysis or sensory deficits in animals. Only mild edema and some fibroblast activation (collagen deposition in epineural space and subperineural region) around nerve fibers were seen in the PRF group at 2 and 7 days after procedure in sciatic nerve and DRG. At 21 days after PRF, these mild changes were back to normal. RF group showed extensive edema, swollen axons and degeneration of neurons [7]. Erdine et al. (2005) reported an animal study showing PRF induced in DRG neurons only, an enlargement of endoplasmic reticulum, and a mild increase of vacuoles. RF showed at the same level mitochondria degeneration, loss of integrity of nuclear membrane, and highly increased number of vacuoles in the DRG cells [8]. These two studies led to the conclusion PRF does not appear to rely on thermal injury to achieve its clinical effect.

One year later, Hamann et al. (2006) applied pulsed radiofrequency to the sciatic nerve or the L5 dorsal root ganglion in the rat. They studied, at up to 14 days after application, the expression of activating transmission factor 3 (ATF3), an early intermediate gene expressed in response to cell stress. They found that ATF3 was upregulated selectively in the small cells of the dorsal root ganglion after direct application to the ganglion but not after application to the sciatic cells. They concluded that pulsed radiofrequency selectively stresses the population containing the nociceptor cell bodies. It would also appear that the primary effect of pulsed radiofrequency is predominantly on the cell body rather than on its processes. The observation that PRF targets preferentially neurons whose axons are composed of small diameters (A-delta and C fibers) was also reported by in this study [9].

It is only in 2009 that publication started reporting more precise neuronal modulation at the ultrastructural level after PRF. Tun et al. (2009) confirmed by ultrastructural approach that CRF (70 °C), as opposed to PRF (42 °C, 120 s), was responsible for much more neurodestruction in the sciatic nerve [10]. Erdine et al. (2009) published interesting results on electronic microscopy of sensory nociceptive axons showing physical evidence of ultrastructural damage following PRF. The mitochondria, microtubules, and microfilaments showed various degrees of damage and disruption. These damages were more important in C fibers than A-delta than A-beta fibers. This observation was consistent with the clinical effect of PRF which seems to have greater effects on the smaller pain-carrying C- and A-delta fibers [11]. Protasoni et al. (2009) also reported some mild effects of PRF on DRGs at the acute phase of exposure. At light microscopy (LM) few differences appeared after PRF, but at transmission electron microscopy (TEM), myelinated axons appeared delaminated and the organization in bundles was lost. Also, T gangliar cells contained abnormal smooth reticulum with enlarged cisternae and numerous vacuoles. As a conclusion authors said PRF slightly damages myelin envelops of nerve fibers at acute stage. No information came out of this study on long-term effect to know whether or not these effects were persistent or just transient [12].

Pulsed radiofrequency may be useful where conventional RF is contraindicated, e.g., neuropathic pain, and it is safe in locations where conventional RF may be potentially hazardous, e.g., DRG lesioning.

PRF is mostly a neuro-remodelling technique based on neuromodulation as opposed to RF which is mainly based on neurodegeneration to reach its clinical effects.

PRF is virtually painless as no heat is generated.

References

Lumbar Facet Denervation

1. Schwarzer AC, Wang SC, Bogduk N, et al. Prevalence and clinical features of lumbar zygapophysial joint pain: a study in an Australian population with chronic low back pain. Ann Rheum Dis. 1995;54:100–6. doi:10.1.136/ard.54.2.100.
2. Wilde VE, Ford JJ, McMeeken JM. Indicators of lumbar zygapophyseal joint pain: survey of an expert panel with the Delphi technique. Phys Ther. 2007;87:1348–61. doi:10.2522/ptj.20060329.
3. Van Zundert J, Vanelderen P, Kessels A, van Kleef M. Radiofrequency treatment of facet-related pain: evidence and controversies. Curr Pain Headache Rep. 2012;16(1):19–25. doi:10.1007/si 1916-011-0237-8. Published online 18 Nov 2011. PMCID: PMC3258411.
4. Cohen SP, Huang JHY, Brummett C. Facet joint pain-advances in patient selection and treatment. Nat Rev Rheumatol. 2013;9(2):101–16. doi:10.1038/nrrheum.2012.198. Advance on lime publication; 20/11/12.
5. van Kleef M, Vanelderen P, Cohen SP, et al. 12. Pain originating from the lumbar facet joints. Pain Pract. 2010;10(5):459–69. The evidence rating used is a system that considers the potential burden and benefit of the treatment.

Physics: Section 1

6. Cosman Jr ER, Cosman Sr ER. Electric and thermal field effects in tissue around radiofrequency electrodes. Pain Med. 2005;6(6):405–24.
7. Sweet WM, Mark VH. Unipolar anodal electrolyte lesions in the brain of man and cat: report of five human cases with electrically produced bulbar or mesencephalic tractotomies. Arch Neurol Psychiatry. 1953;70:224–34.
8. Cosman BJ, Cosman Sr ER. Guide to radio frequency lesion generation in neurosurgery. Burlington: Radionics; 1974.
9. Cosman Sr ER, Cosman BJ. Methods of making nervous system lesions. In: Wilkins RH, Rengachary SS, editors. Neurosurgery. New York: McGraw-Hill; 1984. p. 2490–9.
10. Cosman ER, Rittman WJ, Nashold BS, Makachinas TT. Radiofrequency lesion generation and its effect on tissue impedance. Appl Neurophysiol. 1988;51:230–42.
11. Sluijter ME, Cosman ER, Rittman WJ, Van Kleef M. The effects of pulsed radiofrequency fields applied to the dorsal root ganglion – a preliminary report. Pain Clin. 1998;11(2): 109–18.
12. Ferrante FM, King LF, Roche EA, et al. Radiofrequency sacroiliac joint denervation for sacroiliac syndrome. Reg Anesth Pain Med. 2001;26:137–42.
13. Burnham RS, Yasui Y. An alternate method of radiofrequency neurotomy of the sacroiliac joint: a pilot study of the effect on pain, function, and satisfaction. Reg Anesth Pain Med. 2007;32:12–9.
14. Cosman Jr ER, Gonzalez CD. Bipolar radiofrequency lesion geometry: implications for palisade treatment of sacroiliac joint pain. Pain Pract. 2011;11(1):3–22.

15. Ruiz-Lopez R. Treatment of carpal tunnel syndrome with pulsed radiofrequency. In: Lecture at the invasive procedures in motion conference. Swiss Paraplegic Center, Nottwil; 18–19 Jan 2008.
16. Cosman ER Sr, Cosman ER Jr. RF Electric fields and the distribution of heat in tissue. In: Lecture at the international radiofrequency symposium honoring the 70th birthday of Prof. Menno Sluijter: radiofrequency today. Nottwil; 18–19 Oct 2003.
17. Cosman ER Jr. Physics of radiofrequency. In: Presented at the 15th annual advanced interventional pain conference and practical workshop, and the 17th World Institute of Pain FIPP Examination. Budapest; 31 Aug 2010.
18. Wright RF, Wolfson LF, DiMuro JM, Peragine JM, Bainbridge SA. In vivo temperature measurement during neurotomy for SIJ pain using the Baylis SInergy probe. In: Proceedings of the international spine intervention society 15th annual scientific meeting; Budapest, Hungary. 2007. p. 82–4.
19. Brodkey JS, Miyazaki Y, Ervin FR, Mark VH. Reversible heat lesions with radiofrequency current: a method of stereotactic localization. J Neurosurg. 1964;21:49–53.
20. Dieckmann G, Gabriel E, Hassler R. Size, form, and structural peculiarities of experimental brain lesions obtained by thermocontrolled radiofrequency. Confin Neurol. 1965;26:134–42.
21. Smith HP, McWhorter JM, Challa VR. Radiofrequency neurolysis in a clinical model. Neuropathological correlation. J Neurosurg. 1981;55:246–53.
22. Cosman ER Sr, Cosman ER Jr, Bove G. Blockage of axonal transmission by pulsed radiofrequency fields. In: Proceedings of the society of neuroscience conference. Chicago; 17–21 Oct 2009.
23. Abou-Sherif S, Hamann W, Hall S. Pulsed radiofrequency applied to dorsal root ganglia causes selective increase in ATF-3 in small neurons. In: Proceedings of the peripheral nerve society meeting. Banff; 26–30 July 2003.
24. Buijs EJ, van Wijk RM, Geurts JW, Weeseman RR, Stolker RJ, Groen GG. Radiofrequency lumbar facet denervation: a comparative study of the reproducibility of lesion size after 2 current radiofrequency techniques. Reg Anesth Pain Med. 2004;29(5):400–7.
25. Gultuna I, Aukes H, van Gorp EJ, Cosman ER Jr. Limitations of voltage-controlled radiofrequency and non-temperature-measuring injection electrodes. Submitted for publication; 2011.
26. Cosman Sr ER, Nashold BS, Ovelman-Levitt J. Theoretical aspects of radiofrequency lesions in the dorsal root entry zone. Neurosurgery. 1984;15:945–50.
27. Erdine S, Bilir A, Cosman ER, Cosman ER. Ultrastructural changes in axons following exposure to pulsed radiofrequency fields. Pain Pract. 2009;9(6):407–17.
28. Cosman ER Sr, Cosman ER Jr. RF Electric fields and the distribution of heat in tissue. In: Lecture at the 2nd international symposium on interventional treatment of pain. Swiss Paraplegic Center, Nottwil; 14–15 Jan 2005.
29. Van Zundert J, Patijn J, Kessels A, Lamé I, van Suijlekom H, van Kleef M. Pulsed radiofrequency adjacent to the cervical dorsal root ganglion in chronic cervical radicular pain: a double blind sham controlled randomized clinical trial. Pain. 2007;127(1–2):173–82.
30. Sandkühler J, Chen JG, Cheng G, Randic M. Low frequency stimulation of afferent Aδ-fibers induces long-term depression at primary afferent synapses with substantia gelatinosa neurons in the rat. J Neurosci. 1997;17:6483–91.
31. Bear MF. Bidirectional synaptic plasticity: from theory to reality. Philos Trans R Soc Lond B Biol Sci. 2003;358:649–55.

Physics: Section 2

32. Cosman Jr ER, Cosman Sr ER. Electric and thermal field effects in tissue around radiofrequency electrodes. Pain Med. 2005;6(6):405–24.
33. Cahana A, Vutskits L, Muller D. Acute differential modification of synaptic transmission and cell survival during exposure target position pulsed and continuous radiofrequency energy. J Pain. 2003;4(4):197–202.
34. Erdine S, Yucel A, Cunan A, et al. Effects of pulsed versus conventional radiofrequency current in rabbit dorsal root ganglion morphology. Eur J Pain. 2005;9(3):251–6.

35. Sandkuhler J, Chen JG, Cheng G, Randic M. Low frequency stimulation of the afferent A-delta fibers induces long-term depression at the primary afferent synapses with substantia gelatinosa neurons in the rat. J Neurosci. 1997;17:6483–91.
36. Erdine S, Bilir A, Cosman Sr ER, Cosman Jr ER. Ultrastructural changes in axons following exposure to pulsed radiofrequency fields. Pain Pract. 2009;9(6):407–17.
37. Cosman ER Sr, Cosman ER Jr, Bove G. Blockage of axonal transmission by pulsed radiofrequency fields. In: Proceedings of the society of neuroscience conference. Chicago; 17–21 Oct 2009.

Physics: Section 3

38. Abou-Sherif S, Hamann W, Hall S. Traumatic injury in the PNS induces increased numbers of endoneural mast cells. In: Abstracts 10th world convention on pain. IASP Press. pp 290–1. see also Hamann W, Hall S. RF-lesions in anaesthetized rats. Br J Anaesth. 1992;68:443.
39. Sluijter M, et al. The effects of pulsed radiofrequency fields applied to the dorsal root ganglion – a preliminary report. Pain Clin. 1998;II(2):109–17.
40. Cosman Jr ER, Cosman Sr ER. Electric and thermal field effects in tissue around radiofrequency electrodes. Pain Med. 2005;6(6):405–24.
41. Higuchi Y, Nashold BS, Sluijter M, Cosman E, Pearlstein R. Exposure of the dorsal root ganglion in rats to pulsed radiofrequency currents activates dorsal horn lamina I and II neurons. Neurosurgery. 2002;50(4):850–6.
42. Hamann W. Mechanisms, indications and protocol for pulsed radiofrequency treatment. In: Meeting at St. Thomas' Hospital. London; 2003.
43. Cahana A, Vutskits L, Muller D. Acute differential modulation of synaptic transmission and cell survival during exposure to pulsed and continuous radiofrequency energy. J Pain. 2003; 4(4):197–202.
44. Erdine S, Yucel A, Cimen A, Aydin Podhajsky RJ, Sekiguchi Y, Kikuchi S, Myers RR. The histologic effects of pulsed and continuous radiofrequency lesions at 42°C to rat dorsal root ganglion and sciatic nerve. Spine. 2005;30(9):1008–13.
45. Erdine S, Yucel A, Cimen A, Aydin S, Sav A, Bilir A. Effects of pulsed versus conventional radiofrequency current on rabbit dorsal root ganglion morphology. Eur J Pain. 2005;9:251–6.
46. Hamann W, Abou-Sherif S, Thompson S, Hall S. Pulsed radiofrequency applied to dorsal root ganglia causes a selective increase in ATF3 in small neurons. Eur J Pain. 2006;10:171–6.
47. Tun K, Cemil B, Gurhan A, Kaptanoglu E, Sargon MF, Tekdemir I, Comert A, Kanpolat Y. Ultrastructural evaluation of pulsed radiofrequency and conventional radiofrequency lesions in rat sciatic nerve. Surg Neurol. 2009;72:496–501.
48. Erdine S, Bilir A, Cosman ER, Cosman Jr ER. Ultrastructural changes in axons following exposure to pulsed radiofrequency fields. Pain Pract. 2009;9(6):407–17.
49. Protasoni M, Reguzzoni M, Sangiorgi S, Reverberi C, Borsani E, Rodella LF, Dario A, Tomei G, Dell'Orbo C. Pulsed radiofrequency effects on the lumbar ganglion of the rat dorsal root: a morphological light and transmission electron microscopy study at acute stage. Eur Spine J. 2009; 18:473–8.